
Retinal Vessel Circulation Patterns Visualized From a Sequence of Computer-Aligned Angiograms

Roger Jagoe,* John Arnold,† Christopher Blauth,† Peter L. C. Smith,†
Kenneth M. Taylor,† and Richard Wootton*

Purpose. To present a computer method that can be used to combine the images from a sequence of fluorescein angiograms of the retinal microcirculation so that a composite image can be generated and a color image illustrating circulation at all points in the vascular network can be computed. This should enable more accurate comparison of retinal vascular occlusions that occur during cardiopulmonary bypass surgery.

Methods. Photographic negatives of the macular region from two angiographic sequences, one taken before surgery and the other taken just before the end of bypass, were digitized, background shade corrected, and registered. Composite images were generated as minimum projection images and the filling images generated from parameters of a smooth curve fit to the filling data at every point.

Results. The composite images showed a filling pattern that more accurately reflected the maximum fluorescence at every point than any single image. The images generated from the filling data provide a new way to visualize and quantify changes in the retinal circulation.

Conclusions. The technique demonstrates that problems arising from selection of a single frame from a filling sequence can be overcome by combining images. The technique used to generate the color-coded filling image should prove useful for any image sequence in which differential filling is of interest. Invest Ophthalmol Vis Sci. 1993;34:2881-2887.

A comparison of fluorescein angiograms taken before cardiopulmonary bypass with those taken just before the end of surgery has shown that microvascular occlusions consistent with microembolic events can develop during operation.¹⁻² Subsequent neurologic and intellectual dysfunction have also been observed.³⁻⁴ Because the eye is an outgrowth of the brain it is reasonable to assume that occlusions occurring in the retina also occur in the cerebral microcirculation.

An estimate of the damage in terms of the number of vessel occlusions and the area of nonperfusion can be made by expert human observers. Assessment of these areas requires careful examination and is necessarily subjective. This task can be made more objective using digital image analysis, thus facilitating comparisons among different surgical techniques such as the use of different blood oxygenator types or pharmaco-

logic intervention. In our previous studies,⁵⁻⁶ the choice of frame for analysis was made on the basis of "best capillary filling" from a sequence of about 30 frames from initial arterial filling to late venous drainage. However, this selective method fails to account for information on rates of blood flow and altered circulation around nonperfused areas, which is potentially available in the other frames of the angiographic sequence.

By automatic alignment of the photographic frames in the filling sequence, two benefits can be gained. First, a composite image can be generated showing the maximum fluorescent intensity at every point. Use of this image enables better identification of the capillary network than is possible from a single frame. Second, the time-dependent intensity function is available at every point in the vasculature. This enables blood velocity parameters to be calculated at every point. This information can then be displayed as a color-coded image, where the pixel color represents a filling parameter value at that point.

Blood flow velocity is important in evaluating and monitoring the progression of retinal disorders. In

From the Departments of *Medical Physics and †Surgery, Royal Postgraduate Medical School, London, England.
Submitted for publication August 19, 1992; accepted February 1, 1993.
Proprietary interest category: N.
Reprint requests: R. Jagoe, Department of Medical Physics, Royal Postgraduate Medical School, DuCane Road, London W12 0NN, England.

diabetes, there are factors that might increase or decrease volumetric blood flow, but laser Doppler velocimetry,⁷ blue-light entoptic methods,⁸ and more recently laser scanning ophthalmoscopy⁹ have all confirmed a slowing of the blood velocity in the main vessels and perifoveal capillaries of patients with diabetic retinopathy in comparison with control subjects, and this appears to be progressive. Arend et al⁹ found a reduction in velocity in diabetic patients with no apparent retinopathy.

A practice common to all these methods is the manual selection of regions to measure. The method described in this article enables visualization of blood velocity parameters at all points in the vasculature, and by encoding this information as a color display, where hue represents a dye-dilution parameter, the relative filling patterns in the whole image can be observed.

MATERIALS AND METHODS

Two angiographic sequences were used from one patient: one after aortic cannulation but before the start of bypass, and the other 5 minutes before the heart took over the circulation. The prebypass mean arterial pressure, PO₂, PCO₂ and hematocrit were 85 mmHg, 21.9 kPa, 5.1 kPa, and 40%. The corresponding endbypass parameters were 50 mm Hg, 10.4 kPa, 8.5 kPa, and 33%. Informed consent was obtained from the patient after the nature and possible consequences of the study were explained. The research was approved by the Hammersmith ethics committee and followed the tenets of the Declaration of Helsinki.

Image Acquisition

From each sequence 30–35 photographs were obtained using a Zeiss (Oberkochen, Germany) 30° fundus camera at time intervals of 0.7 seconds starting shortly after an injection of 5 ml of 20% sodium fluorescein into the internal jugular vein. The region photographed was a 30° field centered on the macula. Central areas from each photographic negative in both sequences were scanned using a 50 mm f1.4 Nikkor (Nikon UK Ltd., Surrey, UK) lens attached to a television camera that was connected to a ContextVision (Linköping, Sweden) Gop-302 image analysis computer. The captured image was digitized to a matrix of 512 × 512 8-bit pixels and represented an area of about 7 mm² on the retina. The magnification chosen was such that the resolution was just sufficient to resolve the capillary detail. Some of the images in each sequence were discarded due to blurring resulting from the saline flush used to keep the cornea moist.

Approximate alignment of the prebypass and endbypass images was achieved manually on input by first capturing the prebypass image. The computer display was then set to alternate between showing the cap-

tured prebypass image and the live endbypass image. The live image was adjusted until an approximate match with the captured image was observed. Accurate alignment by this method is difficult but not necessary because automatic registration was achieved at a later stage. However, approximate alignment was required to ensure that the spatial differences between corresponding image regions was small, i.e., not more than 20 pixels anywhere in the image (this information was used in the ensuing automatic registration procedure); and there was a nearly full common frame between images to process subsequently.

Computer Preprocessing

Three preprocessing stages were required before the images in a sequence could be combined and the filling pattern computed. These were background shade correction, background equalization, and spatial alignment of all the images in a sequence. Shade correction and background equalization were carried out as described previously.⁶

Approximate alignment of the images was ensured by the method of capture, but this was not sufficient to allow accurate superimposition of the images. Accurate geometric registration was achieved by automatic alignment of all the images in a sequence to a selected reference image from the sequence (any image around midsequence showing reasonable filling was adequate for this purpose). The method relied on finding matching regions between an image and the reference image and was an adaptation of a previous technique⁶ modified to overcome the difficulties of locating vessel branches in poorly filled early frames. The coordinates of the centers of the matching regions were used to generate two polynomials, which in turn were used to warp each image in the sequence to the reference image.

RESULTS

Composite Image

The difficulties that can arise from selection of a single frame from the filling sequence are illustrated by an examination of the filling pattern along a length of one of the capillaries in the prebypass sequence. A close-up of the selected capillary is shown in Figure 1. The four windows show the same capillary at successive time intervals of 0.7 seconds. The plots to the right of each window show the image grey level values along the capillary track from left to right between the indicated arrows. These values were derived from a program that enabled an observer to mark a track along a length of vessel. The program then computed a region that formed a narrow band along and parallel to the drawn track. This region was then digitally stretched to

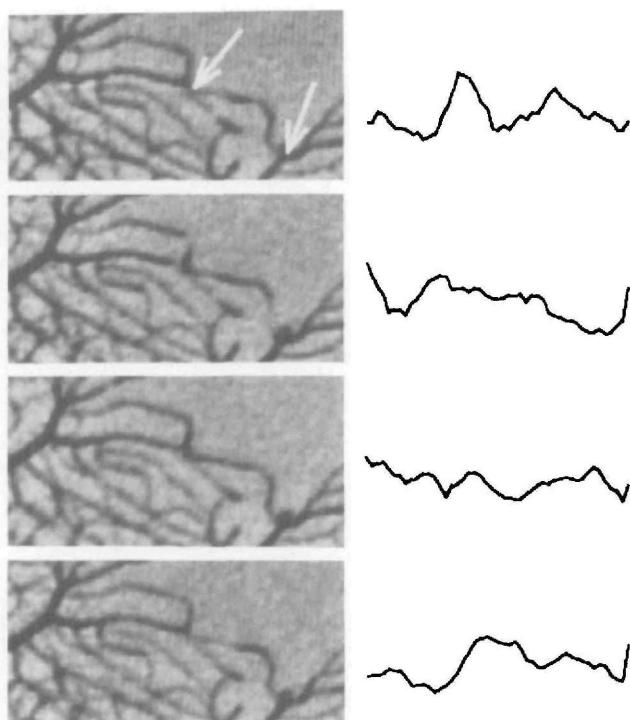


FIGURE 1. A close-up view of the changes in fluorescein filling in one capillary at intervals of 0.7 seconds. The plot to the right of each image show the inverted grey levels—representing fluorescence, along the capillary between the points indicated by the arrows.

form a narrow rectangular block in which the capillary ran from one end to the other. The minimum grey level path along the block was located subject to the conditions that it advanced 1 pixel along the block and not more than 1 pixel sideways at each step. This removed any variation due to observer differences in marking the track. As can be seen, the fluorescein pattern changes abruptly, probably because of red blood cell aggregates. The optimally filled frame could be selected from any of these frames, but each would show a different pattern of fluorescence at the small capillary level.

The problems caused by changing filling patterns when making image comparisons can be overcome by creating composite images. A single composite image was generated from each sequence by geometrically aligning all the images in the sequence and a new image was computed by selecting at each image position, the minimum grey value (maximum filling) at that point for all images in the sequence. The resulting composite image showed the maximum fluorescence at all points in the macula. The composite images derived from the prebypass and endbypass sequences are shown in Figures 2 and 3. These show features in the microvascular structure not evident from any individual image selected on the basis of optimal filling.

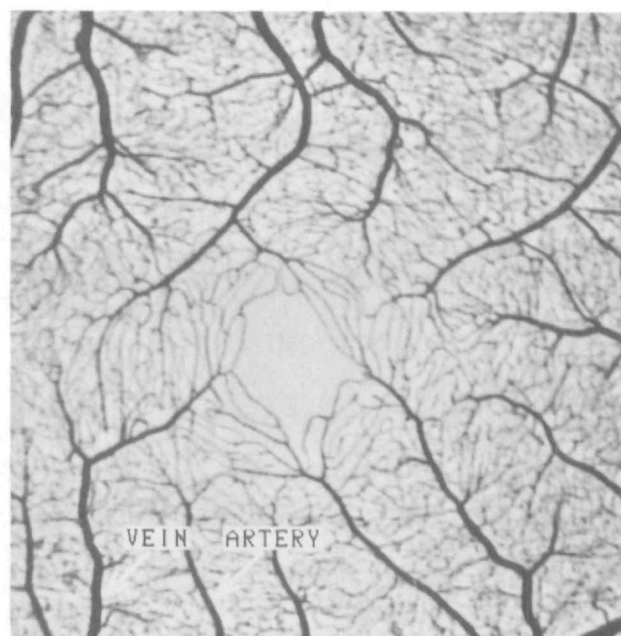


FIGURE 2. Prebypass composite image.

Time to Maximum Filling Image

Segmentation of the Vascular Structure. A grey-level threshold value was computed from the composite image such that the darkest 25% of the image area was below this value. All of the vascular structure was included in the region resulting from segmentation at this grey value. This binary image mask defined areas where subsequent processing of the time-dependent information was performed.



FIGURE 3. Endbypass composite image.

Calculation of Time to Maximum Filling. For each point in the region defined by the vascular mask, the grey-level values can be plotted against time. The variation in grey level with time is illustrated in Figure 4 for the points indicated by the arrows in Figures 2 and 3, one in an artery and the other in a vein. Plots are shown for both the prebypass and endbypass filling sequences. It is clear that the raw data points form a noisy plot making it difficult to estimate accurately the time to maximum filling. However by fitting smooth curves to the data using third-order polynomials, the time to maximum filling was estimated at each point in the vascular structure. This time was 20.3 and 33.2 seconds for the arterial point indicated in the prebypass and endbypass sequences, respectively, and 22.2 and 36.3 seconds for the point in the vein. The onset of filling was delayed in the endbypass sequence by about 12 seconds because of the extra path length of the bypass circuit. The delay between the peak arterial and venous filling was 1.9 seconds in the prebypass sequence and 3.1 seconds in the endbypass sequence. This could be attributable to multiple factors such as hemodilution by the priming fluid in the pump system and changes to blood pressure, O_2 and CO_2 tension, all of which affect autoregulation and therefore blood velocity.

A new image was then generated in which the pixel grey levels represented the time to maximum filling at each point in the vascular structure. The grey levels for the endbypass image were calculated from the elapsed time in tenths of a second from the first appearance of fluorescein in the retinal vessels. A similar image was computed from the prebypass sequence. However, to compare both images, they must be registered accurately in time, and a guess at the onset of filling is not accurate enough to allow this. Even if it were possible, the time difference is not constant over all the image. Registration of the prebypass filling image to the endbypass image was done by calculating the mean time of maximum filling for both images and correcting for the difference by an additive time constant to the prebypass image. These parametric images are best viewed using pseudo-color (Figures 5 and 6) where color is coded to represent elapsed time. The time scale to the left represents an interval of about 2.5 seconds, so each color band represents approximately 0.5 seconds. The yellow regions show late-filling capil-

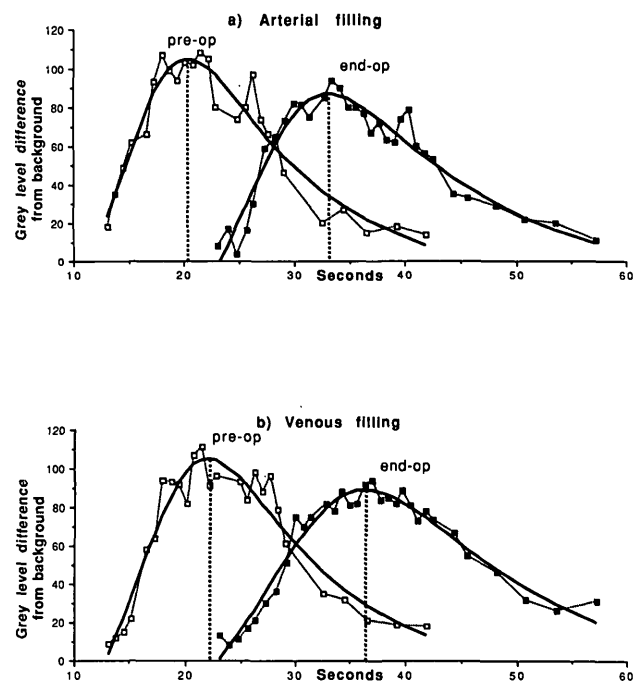


FIGURE 4. Dye dilution data for the two points indicated for the prebypass and endbypass filling sequences. Polynomial curves fitted to the data enable an estimate of the time to maximum filling at each point in the vascular structure.

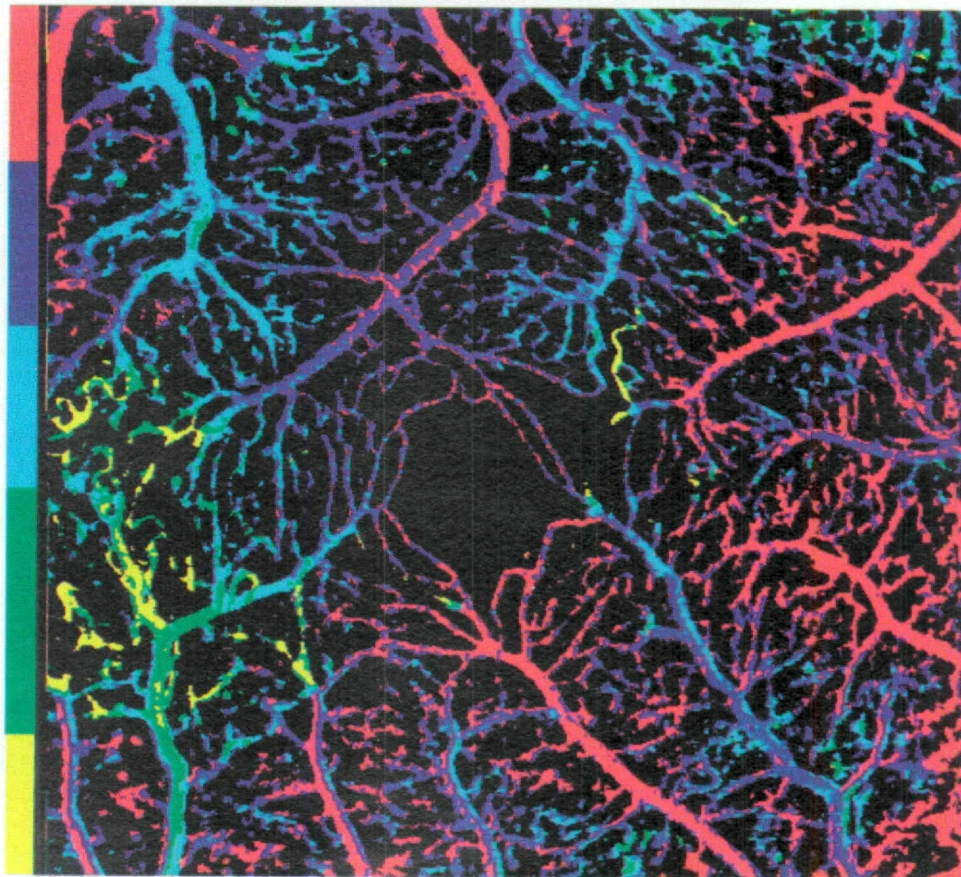
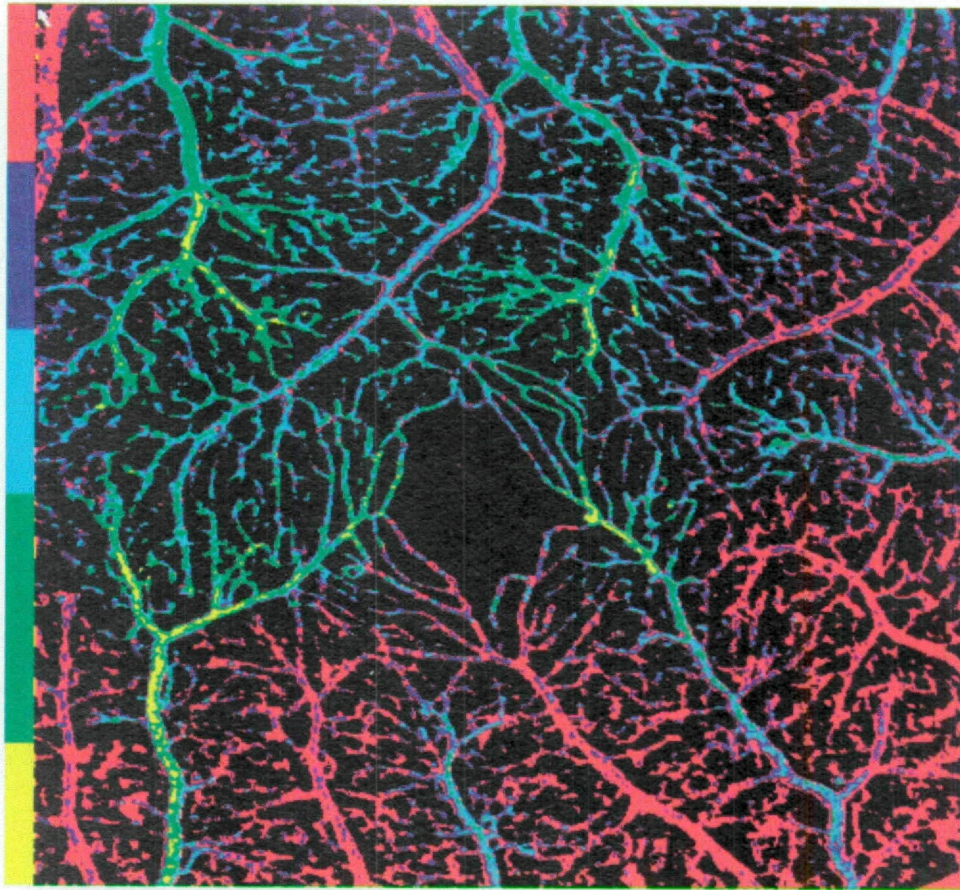
laries. A comparison of the region to the lower left of center shows many late-filling vessels in the endbypass image surrounding a region of nonperfusion. This is a typical example of a temporary occlusion that occurs during bypass and is assumed to be microembolic in origin. Another typical region of capillary drop-out can be seen in the upper right of center. In addition, there are a few late-filling vessels that are clearly indicated in other regions that would not normally be counted as nonperfused regions.

DISCUSSION

In previous epidemiologic studies, areas of nonperfusion were defined by comparison of two well-filled frames selected from the prebypass and postoperative sequences. This method, which relied on comparison of single frames, could not distinguish between late-filling capillaries and nonfilling capillaries. It is apparent from Figure 6 that late-filling capillaries occur ad-

FIGURE 5. A parametric image of the time to maximum filling for the prebypass sequence. The pixel values displayed in pseudo-color represent the time to maximum filling at each point. The scale represents a time interval of about 2.5 seconds. Late-filling capillaries are shown by the lighter green and yellow colors.

FIGURE 6. The equivalent color-coded image for the end-bypass sequence. The mean time has been synchronized with Figure 5 and time interval is the same.



adjacent to the regions of nonperfusion. However, there are examples of late-filling capillaries that appear to occur in isolation, the significance of which is not yet clear. Use of the composite and time-filling images enables independent assessment of nonfilling and late-filling capillaries.

Normal filling of the small capillaries is not continuous as was shown by the filling pattern of a single capillary monitored over a period of 2.1 seconds. At any one time, small lengths appeared to be almost devoid of fluorescence. Thus a comparison of two angiograms using single time slice images could result in identification of missing sections of capillary giving rise to false-positives. This potential inaccuracy can be overcome by a comparison that uses the composite images.

Similar patterns of low- and high-density fluorescein have been observed in capillaries by Wolf et al¹⁰ using a video scanning laser ophthalmoscope. They attributed the low-density segments to erythrocytes (rouleaux formations) and the high-density segments to cell-free plasma, and were able to track the movement of these segments to measure blood velocity in the capillaries.

Although the filling pattern as shown by the raw data values in Figure 4 is noisy, the overall pattern is well represented by third-order polynomials around the point of maximum filling. These curves are clearly not the most suitable model to use in fitting the data and would not be appropriate to use in estimating other parameters such as rate of filling or mean transit time. Estimation of these parameters is critically dependent on how well the curve fits the data in the early and late stages of filling. However, it is reasonable to assume that the time to maximum filling is less sensitive to the model used as any method that approximated the filling data near the peak values would give a similar estimate. Another advantage of using the peak filling time is that it is minimally affected by nonlinearities in the relationship between the grey-level values and dye concentration.

Dye-dilution curves obtained from angiographic photographic sequences have been used for many years to estimate mean circulation times and used in conjunction with measured vessel diameters to estimate blood flow.¹¹⁻¹² The estimation of the mean transit time cannot be made without making some assumptions and fitting a model to the data. The standard method of fitting the down slope of the curve plotted on log-linear paper with a straight line can be inaccurate, especially in venous curves. If recirculation begins early in the drainage phase, there may be an insufficient number of straight line points to estimate the slope with confidence. Assumptions about the linearity of the relationship between the digitized grey levels and the dye concentration must also be made.¹³ Other

models that have been used to fit dye-dilution curves are the lagged-normal model,¹⁴ the log-normal model and the gamma-variate curve.¹⁵ Riva et al¹³ report good fits with the log-normal model for both arterial and venous dilution curves. This technique requires estimation of several parameters from the experimental data, but it is not clear how noisy data affect the parameter estimations or how well the model can be applied to data from pathologic cases, in which the drainage is slow or staining of the vessel wall occurs. There is also the difficulty of applying models to filling data from capillaries, where the filling curve is flatter and more affected by discrete segments of fluorescein. Estimation of the time to peak filling requires few assumptions and is relatively robust. Although it cannot be used as easily as mean transit time to estimate blood flow, it can be used to follow the progression of disease and to make quantitative comparisons of patient populations.

It is not known how choroidal non-perfusion might affect the results. It would certainly have some effect on the background image correction and may therefore influence the vessel detection algorithms. More studies should investigate the effect of uneven choroidal filling on estimates of maximum filling in retinal vessels. Video angiography,¹⁶⁻¹⁸ two-point fluorophotometry,¹⁹ and more recently, laser scanning ophthalmoscopy¹⁰ have enabled the sampling rate to be increased but the extraction of the time sequence information has been hindered by problems of registration and manual selection of sampling points. Nagin et al²⁰ used registered images of the optic disc to measure filling rates in points inside the disc, and by setting a filling-rate threshold was able to segment regions of abnormal filling. They also measured filling rates from manually selected points in the large vessels near the disc.

The advantages of the technique described here are that it is totally automatic, all points in the vasculature are examined individually, and the time-coded color image summarizes at a glance the relative patterns of filling. By selecting a suitable time threshold it is possible to make a quantitative estimation of late-filling vessels. By comparing two composite images, those capillaries that remain unfilled throughout the complete sequence can be identified more accurately than by a comparison of single frames. By comparing two time-coded images it is possible to detect changes in filling patterns providing the images are synchronized. It is not possible to synchronize accurately using the injection time, so it is necessary to estimate a relative time from the images themselves. In this study, the times were synchronized from the mean peak filling along the midline of the main vessels. Other techniques of synchronization may be appropriate for different applications, such as the time of first appear-

ance of the dye as calculated from the slope of the arterial dye-dilution curve. Quantification of late-filling capillaries in the particular case of bypass patients should account for changes in the transit time that occurs during surgery.

To obtain sufficient resolution to visualize the smallest capillaries around the macula with a 512×512 pixel imaging system, only a small portion of the fundus image was processed. A matrix of at least 2200×2200 pixels would be required to digitize an entire negative at the same resolution and the corresponding increase in processing and storage capabilities would be considerable.

This new technique can be used to detect and measure capillary dropout during cardiopulmonary bypass. It also provides information on retinal circulation and has the advantage that it can be applied to existing photographic angiographic sequences.

Key Words

image analysis, fluorescein angiograms, retinal circulation, non-perfusion.

Acknowledgment

This work was supported in part by the British Heart Foundation.

References

1. Blauth C, Arnold J, Kohner EM, Taylor KM. Retinal microembolism during cardiopulmonary bypass demonstrated by fluorescein angiography. *Lancet ii*. 1986; 837-839.
2. Dutton RC, Edmunds LH Jr, Hutchinson JC, Roe BB. Platelet aggregate emboli produced in patients during cardiopulmonary bypass with membrane and bubble oxygenators and blood filters. *J Thorac Cardiovasc Surg*. 1974;67:258-265.
3. Taylor KM. Pathophysiology of brain damage during open heart surgery. *Texas Heart Institute J*. 1986; 13:91-96.
4. Breuer AC, Furlan AJ, Hanson MR, et al. Neurologic complications of coronary artery bypass surgery. *Cleveland Clin*. 1981;48:205-206.
5. Jagoe JR, Blauth CI, Smith PL, Arnold JV, Taylor KM, Wootton R. Quantification of retinal damage during cardiopulmonary bypass: comparison of computer and human assessment. *IEE Proceedings Pt I*. 1990; 137:170-175.
6. Jagoe JR, Arnold J, Blauth C, Smith PLC, Taylor KM, Wootton R. Measurement of capillary drop out in retinal angiograms by computerised image analysis. *Pattern Recognition Letters* 1992;13:143-151.
7. Grunwald JE, Riva CE, Sinclair SH, Brucher AJ, Petrig BL. Laser doppler velocimetry study of the retinal circulation in diabetes mellitus. *Arch Ophthalmol*. 1987;104:991-996.
8. Rimmer T, Fallon TJ, Kohner EM. Long term follow-up of retinal blood flow in diabetes using the blue field entoptic phenomenon. *Br J Ophthalmol*. 1989;73:1-5.
9. Arend O, Wolf S, Jung F, et al. Retinal microcirculation in patients with diabetes mellitus: dynamic and morphological analysis of perifoveal capillary network. *Br J Ophthalmol*. 1991;75:514-518.
10. Wolf S, Arend O, Toonen H, Bertram B, Jung F, Reim M. Retinal capillary blood flow measurement with a scanning laser ophthalmoscope. *Ophthalmology*. 1991;98:996-1000.
11. Hickam JB, Frayser R. A photographic method for measuring the mean retinal circulation time using fluorescein. *Invest Ophthalmol Vis Sci*. 1965;1:876-884.
12. Bulpitt CJ, Dollery CT. Estimation of retinal blood flow by measurement of the mean circulation time. *Cardiovasc Res*. 1971;5:406-412.
13. Riva CE, Fekete GT, Ben-Sira I. Fluorescein dye-dilution technique and retinal circulation. *Am J Physiol*. 1978;234:H315-H322.
14. Bassingthwaite JB, Ackerman FH, Wood EH. Applications of the lagged normal density curve as a model for arterial dilution curves. *Circ Res*. 1966;18:398-415.
15. Thompson HK Jr, Starmer CF, Whalen RE, McIntosh HD. Indicator transit time considered as a gamma variate. *Circ Res*. 1964;14:502-515.
16. Jung F, Kiesewetter H, Korber N, Wolf S, Muller G. Quantification of characteristic blood flow parameters in the vessels of the retina with picture analysis system for video fluorescence angiograms: initial findings. *Graefes Arch Ophthalmol*. 1983;221:133-136.
17. Fonda S, Bagolini B. Relative photometric measurements of retinal circulation (dromofluorograms). *Arch Ophthalmol*. 1977;95:302-307.
18. Preussner PR, Richard G, Darrelman O, Kreissig I. Quantitative measurement of retinal blood flow in human beings by application of digital image processing methods to television fluorescein angiograms. *Graefes Arch Ophthalmol*. 1983;221:110-112.
19. Eberli B, Riva CE, Fekete GT. Mean circulation time in retinal vascular segments. *Arch Ophthalmol*. 1979; 97:145-148.
20. Nagin P, Schwartz B, Reynolds G. Measurement of fluorescein angiograms of the optic disc and retina using computerised image analysis. *Ophthalmology*. 1984;92:547-552.